

# Spin diffusion from an inhomogeneous quench in an integrable system

Marko Ljubotina, Marko Žnidarič, and Tomaž Prosen\*  
Physics Department, Faculty of Mathematics and Physics,  
University of Ljubljana, Jadranska 19, SI-1000 Ljubljana, Slovenia

Nonequilibrium dynamics of integrable quantum systems is one of the main current focuses of both theoretical and experimental condensed matter physics [1]. A macroscopic number of conservation laws existing in such systems [2] provide a variety of ways to break ergodicity, manifesting, for instance, in equilibration processes to non-thermal states or ballistic high-temperature transport of conserved quantities, such as energy, magnetisation or charge. Recently, a generalisation of hydrodynamics has been put forward [3, 4] which successfully predicts ballistic currents and scaled density profiles of integrable interacting systems quenched from inhomogeneous initial states [5–7]. However, when ballistic transport is prohibited due to generic symmetries, such as is the case for spin transport in the anisotropic Heisenberg spin chain in the easy axis (Ising) regime, this theory makes no prediction. Here we propose a conjecture, based on large scale simulations, that a quench from an inhomogeneous initial state will in such cases generically result in diffusive spin dynamics. Remarkably, in the case of isotropic Heisenberg interaction, spin relaxation is super-diffusive but with universal scaling dynamics which obey the standard diffusion equation in nonlinearly scaled time.

Integrable models form cornerstones of our understanding of nature, be it e.g. the classical Kepler problem, harmonic oscillators, the planar Ising model, etc. Their equilibrium physics is usually well understood, even for the most complicated among integrable models, e.g. the ones solvable by the Bethe ansatz [8]. Nonequilibrium physics of quantum systems on the other hand is much less understood [9], particularly when going beyond the simplest integrability of quadratic models. This gaping theoretical hole is becoming even more apparent with the advancement of experimental methods that are offering us analog simulation of models beyond the capability of our best theoretical and numerical methods [10, 11].

Relaxation and nonequilibrium transport can be conveniently studied by quenching an extended system, say in one-dimension, from an inhomogeneous initial state [5–7], meaning that, initially, the system is prepared in the state where the left and the right part, for  $x < 0$  and  $x > 0$  respectively, are in different equilibrium states, and then at  $t = 0$ , the system is let to evolve with a homogeneous interacting Hamiltonian. A naive classical reasoning might be that, because integrable systems are

distinguished by constants of motion that force the dynamics to be “simple and periodic” (e.g., orbits winding up the torus), one should expect to see ballistic transport. We shall demonstrate that this picture, while being correct for trivially integrable noninteracting models, such as harmonic oscillator chains [12], can in fact be wrong for an interacting quantum integrable model.

In extended interacting integrable system a macroscopic number of local conservation laws exists, in number proportional to the number of degrees of freedom, which can be exploited to develop *generalised hydrodynamics* [3]. This theory for typical inhomogeneous initial states predicts ballistic scaling  $f(\xi = x/t)$  of densities and currents of conserved quantities, such as energy, charge or magnetisation. However, in systems with parity ( $\mathbb{Z}^2$ ) symmetries, such as particle-hole exchange or spin reversal, observables that are odd under the parity and initial states that are symmetric under the combined parity and spatial reflection  $x \rightarrow -x$ , the ballistic contribution to transport can vanish and then the quasi-particle formalism [3, 4] makes no prediction. This means that the transported conserved quantity at  $x = 0$  grows slower than linear with  $t$ . Because the parity symmetry is ubiquitous, our setup should be widely applicable. We demonstrate our results on the anisotropic Heisenberg chain ( $XXZ$  model), being an important theoretical model. However, we stress that the  $XXZ$  model goes beyond being a mere toy model – it has been instrumental in the development of quantum integrability [13, 14] and describes interaction in real spin chain materials [15]. Our results thus reveal a surprising property of an important integrable model as well as pose a challenge to theories which at present are unable to account for our observations.

The Hamiltonian of the  $XXZ$  chain of  $n$  sites reads

$$\mathcal{H} = J \sum_{x=-n/2}^{n/2-1} (s_x^x s_{x+1}^x + s_x^y s_{x+1}^y + \Delta s_x^z s_{x+1}^z) , \quad (1)$$

where  $\Delta$  is the anisotropy parameter and  $s_k^\gamma = \frac{1}{2}\sigma_k^\gamma$  are the spin 1/2 operators expressed in term of Pauli matrices  $\sigma_k^\gamma$  (we use units  $J = \hbar = 1$ ). The Hamiltonian preserves the total magnetisation,  $M = \sum_x s_x^z$ ,  $[\mathcal{H}, M] = 0$ . We are going to study the spin transport satisfying the continuity equation  $ds_x^z/dt = j_{x-1} - j_x \approx -\nabla j_x$  with the current

$$j_x = s_x^x s_{x+1}^y - s_x^y s_{x+1}^x . \quad (2)$$

The existence of spin-reversal parity  $S = \prod_x \sigma_x^x$ ,

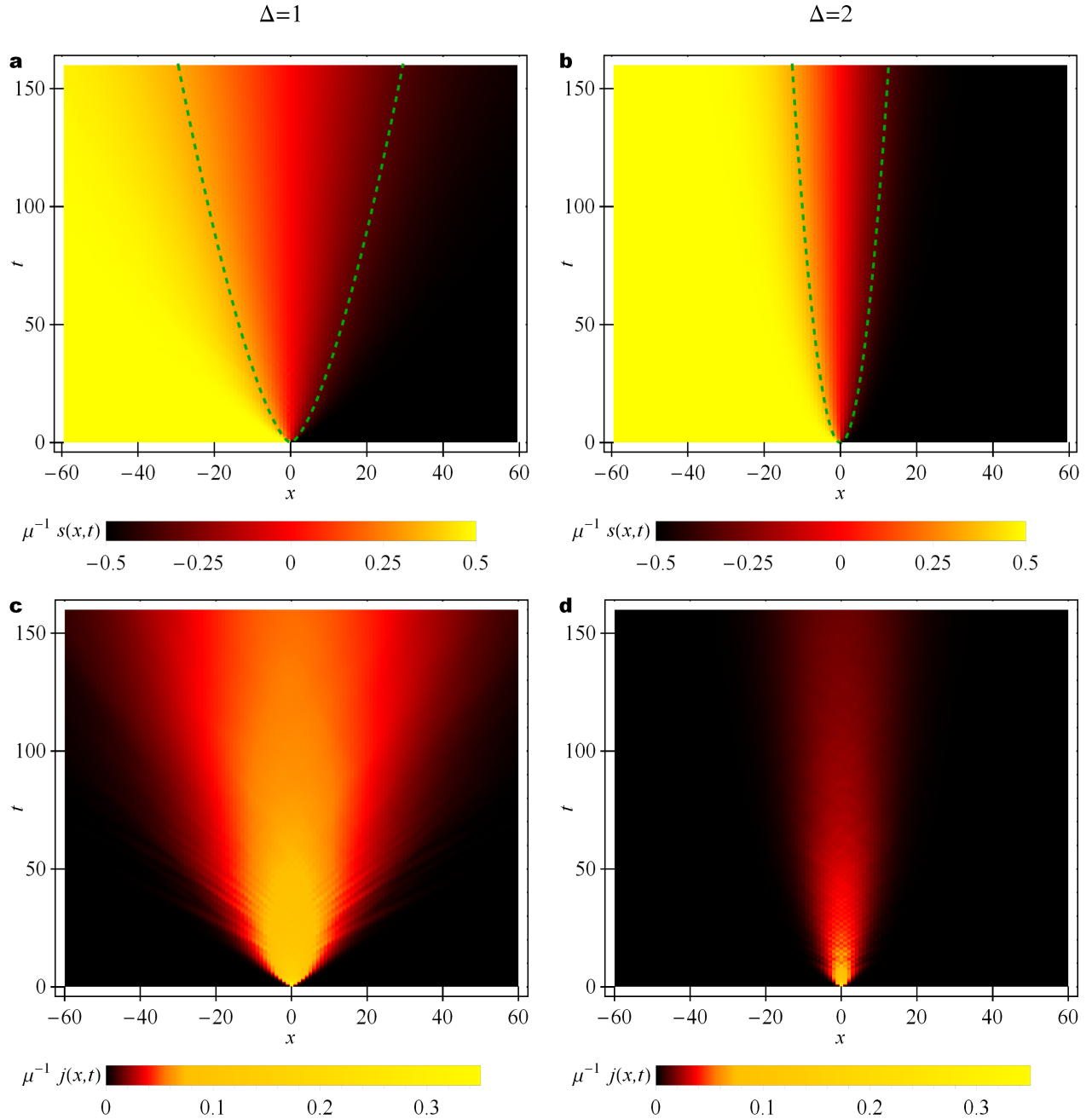


Figure 1. Time evolution of spin density  $s(x,t) = \text{tr}(\rho(t)s_x^z)$  (top row) and current (bottom row) profile  $j(x,t) = \text{tr}(\rho(t)j_x)$  for the isotropic point  $\Delta = 1$  (left column), and  $\Delta = 2$  (right column), following an inhomogeneous quench. One can see that the spreading is much faster for  $\Delta = 1$ , in both cases though it is slower than ballistic. Dashed curves guide the eye towards scaling  $x \sim t^{1/2}$  in (a), and  $x \sim t^{2/3}$  in (b). Data are shown for  $n = 320$  and small initial polarisation  $\mu = \pi/1800$ .

$[\mathcal{H}, S] = 0$ , and odd current  $j_x S = -S j_x$ , implies an absence of ballistic transport channels based on local conserved charges [16]. We are going to simulate the time evolution of an initial inhomogeneous state composed of two halves with opposite magnetisations. To this end we choose a product initial state described by a density

operator  $\rho$ ,

$$\rho(t=0) \sim (1 + \mu \sigma^z)^{\otimes \frac{n}{2}} \otimes (1 - \mu \sigma^z)^{\otimes \frac{n}{2}}, \quad (3)$$

where the parameter  $\mu \in [-1, 1]$  determines the initial magnetisation, being  $\langle s_{x \geq 0, < 0}^z \rangle = \pm \frac{1}{2} \mu$ . Each of the initial halves can be thought of as being in equilibrium state  $\sim e^{\pm h \sum_x s_x^z}$  at very high temperature and finite magneti-

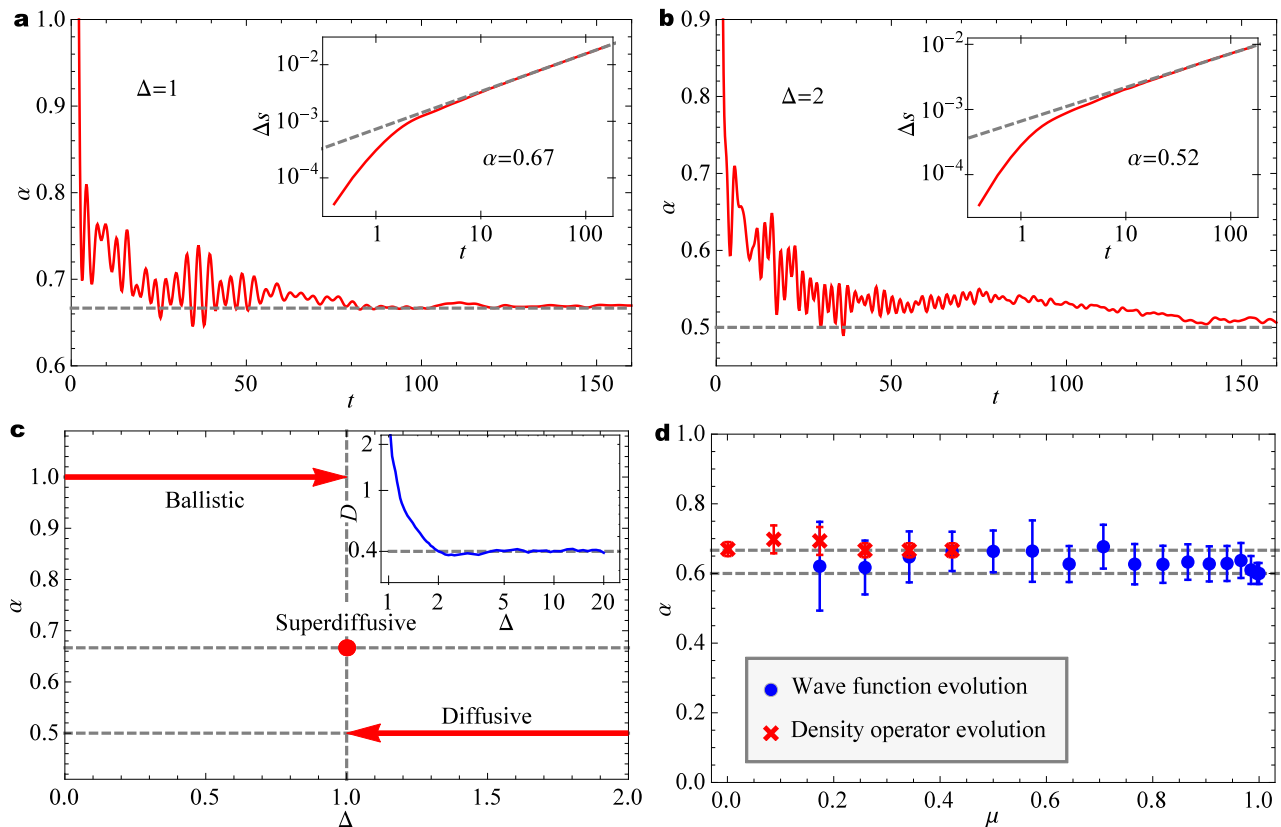


Figure 2. Scaling exponent  $\alpha$  of magnetisation spreading,  $\Delta s \propto t^\alpha$ . (a, b) Local exponent  $\alpha(t)$  calculated as a numerical log-derivative  $d \log \Delta s(t) / d \log t$  for  $\Delta = 1$  (a) and  $\Delta = 2$  (b) (dashed lines indicate exponents  $2/3$  and  $1/2$ , resp., while dashed lines in the insets show best power-law fits to  $\Delta s(t)$  – red curve), both for  $\mu = \pi/1800$ . (c) Conjecture for the dependence  $\alpha(\Delta)$  at high temperatures and small  $\mu$ . The inset shows the diffusion constant obtained from Fick’s law for various values of  $\Delta$  in the diffusive regime, converging to a finite value at large  $\Delta$  (agreeing with Ref. [23]). (d) Dependence on  $\mu$  for  $\Delta = 1$  shows a small but significant change in the behaviour: for  $\mu \approx 1$  it is closer to  $\alpha = 3/5$  while for small  $\mu$  it becomes significantly close to  $\alpha = 2/3$  (dashed). For intermediate  $\mu$  the error-bars are larger since the simulation becomes less efficient there (see Methods).

sation. We are therefore studying high-energy nonequilibrium physics of the model. While the initial state is pure for  $|\mu| = 1$  (a fully polarised domain wall), evolution of which has been studied in the past [17], the choice of a mixed state offers several important advantages: it is generic and not plagued by the speciality of  $\mu = 1$  at  $\Delta > 1$  for which the dynamics freezes due to the proximity to a gapped eigenstate [18], and it is, for small  $\mu$ , better suited for numerical simulations. We also mention that such an initial state can be thought of as representing an ensemble of pure states with randomised angle  $\varphi$  on the Bloch sphere (see Methods).

We focus our efforts on  $\Delta \geq 1$  where there are no analytic results known for the magnetisation transport, and the method [3, 4] only predicts vanishing ballistic contribution. Two representative examples of a time evolved state  $\rho(t)$ , namely the spin and current profiles  $s(x, t) = \text{tr} \rho(t) s_x^z$ ,  $j(x, t) = \text{tr} \rho(t) j_x$ , are shown in Fig. 1. In order to obtain the exact type of transport we shall quantitatively study equilibration of magnetisation, in particular the scaling of spin and current profiles

as well as the transferred magnetisation between the two halves, whose asymptotic scaling power  $\alpha$  characterizes the transport type,

$$\Delta s(t) = \int_0^t j(0, t') dt' \propto t^\alpha, \quad (4)$$

where  $j(0, t)$  is the current at the half-cut. For  $\alpha = 1/2$  the transport is diffusive, for  $1/2 < \alpha < 1$  it is called superdiffusive, and finally,  $\alpha = 1$  corresponds to ballistic transport. We evolved the initial state  $\rho(0)$  (3) up to long times (of order  $t \approx 160$ ) and set large enough  $n$  so that there was no significant finite size effects. From the data we then infer the exponent  $\alpha$  using Eq.(4), see Fig.2(a) and (b) for representative plots. Dependence of the exponent  $\alpha$  on  $\Delta$  is summarised in Fig. 2(c). While the transport is found to be ballistic for  $\Delta < 1$ , expectedly so for the integrable system, also known rigorously [19], at  $\Delta \geq 1$  we find rather clear non-ballistic relaxation. In particular, at  $\Delta = 1$  it is superdiffusive while for  $\Delta > 1$  the transport is diffusive, observed in driven steady-state setting [20, 21] as well as in the Hamiltonian one [22–

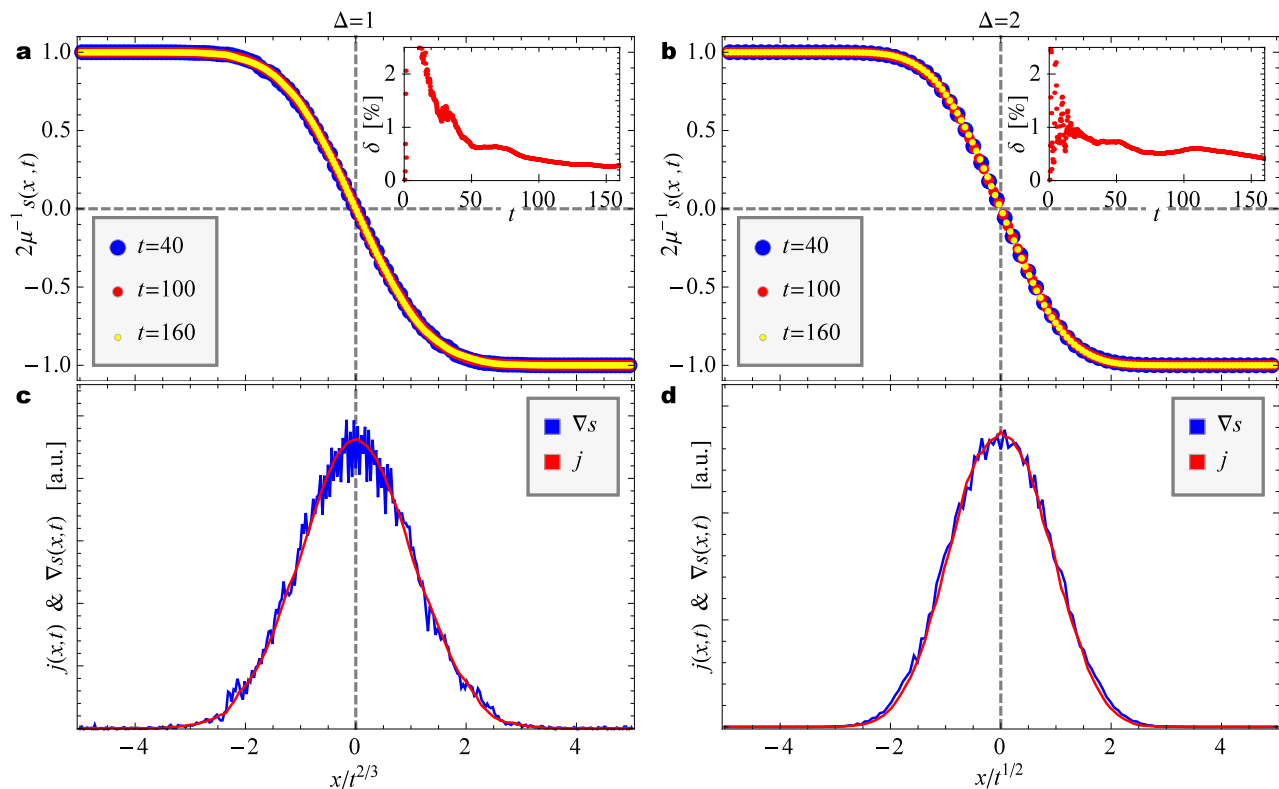


Figure 3. Scaling of density and current profiles with  $x/t^\alpha$ . In the top row we show the scaling of magnetisation profiles, (a) for  $\Delta = 1$  using  $\alpha = 2/3$ , and (b) for  $\Delta = 2$  and using  $\alpha = 1/2$  (note that the points for different times overlap almost perfectly; the insets show the convergence of the relative root-mean-square difference (in %) between data  $s(x, t)$  and scaled erf-profiles (see text) as a function of time). Frames (c) and (d) show the emergence of Fick's law at late times (shown at  $t = 160$ ), comparing current profiles (red) to gradients of spin density (blue) – both indistinguishable from Gaussians, for  $\Delta = 1$  in (c) and  $\Delta = 2$  in (d). In all plots the system size is  $n = 320$ .

25]. At  $\Delta = 1$  we also observe small dependence of  $\alpha$  on  $\mu$ . While for small  $\mu$ , i.e., small deviations from an infinite temperature state  $\sim \mathcal{K}$ , the exponent is close to  $2/3$ , closer to pure state  $\mu = 1$  it appears to be closer to  $\approx 3/5$  (we note that a different numerical procedure is used in the two regimes, see Methods).

The scaling of the transferred magnetisation unequivocally shows a surprising non-ballistic transport in an integrable system. But we can do more still. In Fig. 3 we demonstrate that the spin profiles can be described by a function of a single scaling variable  $x/t^\alpha$  – profiles at large times collapse to a single curve. In addition, the profiles of current and magnetisation are proportional to each other at different times (Fig. 3(c,d)), therefore validating Fick's law  $j = -D\nabla s$  where the behaviour of the diffusion constant  $D$  with respect to the anisotropy is shown in the inset of Fig. 2(b). This comes as no surprise in the diffusive regime  $\Delta > 1$  where the scaling function of the magnetisation (Fig. 3(b)) is simply the error function  $s(x, t) = -\frac{\mu}{2}\text{erf}(x/\sqrt{4Dt})$ . However, the same can not be said for the isotropic point  $\Delta = 1$ . Proportionality between the magnetisation gradient and the current profile (Fig.3(c)), this time with a time-dependent ratio

$D \simeq \frac{K}{3}t^{1/3}$ , suggests a diffusion equation in a scaled time

$$\frac{\partial s(x, t)}{\partial \tau} = \frac{K}{4} \frac{\partial^2 s(x, t)}{\partial x^2}, \quad \text{where } \tau = t^{4/3}, \quad (5)$$

which again yields error function profile with a different scaling variable  $s(x, t) = -\frac{\mu}{2}\text{erf}(K^{-1/2}x/t^{2/3})$  with  $K = 2.30 \pm 0.03$ . In Fig.3(a) we compare numerical profiles with the error function, again finding good agreement within accuracy of our simulations. Therefore, the scaling function is, in both cases,  $\Delta = 1$  and  $\Delta > 1$ , the error function, the difference being only in the scaling variable which is  $x/t^{2/3}$  at the superdiffusive isotropic point. This result is surprising, as anomalous diffusion is usually associated with Levy processes and hence long (non-Gaussian) tails in the profiles. Here it seems it all amounts to a nonlinear rescaling of time. Theoretical explanation of this effect is urgent.

Lastly, we mention a numerical observation that explains why we can simulate dynamics to such long times, and is an interesting property on its own. We use a time-dependent density matrix renormalisation group method (tDMRG), see Methods. The efficiency

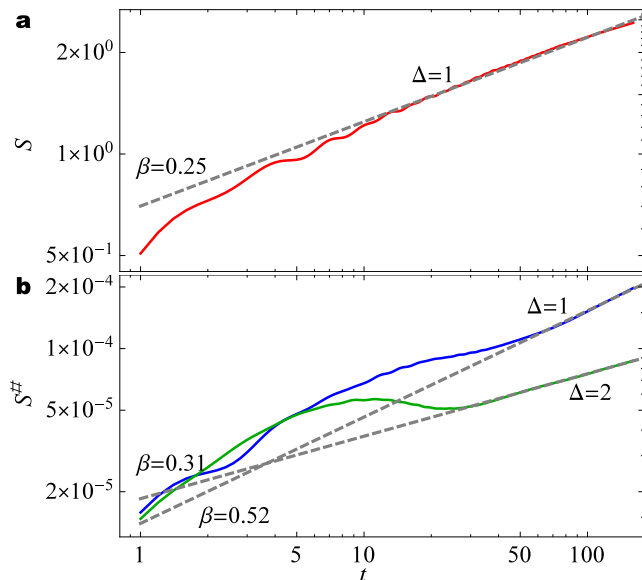


Figure 4. Complexity of  $\rho(t)$  grows unusually slowly as  $\sim t^{\beta}$ . (a) Von Neumann entanglement entropy  $S$  for the fully polarized initial state ( $\mu = 1$ ) at the isotropic point. (b) Operator space entanglement entropy  $S^{\#}$  for  $\Delta = 1$  (blue) and  $\Delta = 2$  (green), both for  $\mu = \pi/1800$ . Bipartition into two equal halves and a system size of  $n = 320$  are used.

of tDMRG depends on the entanglement entropy, i.e., for pure state evolution on the Von Neumann entropy  $S = -\text{tr}[\rho_A \ln \rho_A]$  of the reduced state  $\rho_A = \text{tr}_B |\Psi\rangle\langle\Psi|$ , whereas for mixed states evolution on an analogous operator space entanglement entropy  $S^{\#}$  [26] of a vectorised density operator  $\rho$ . When starting with a typical product initial state both entropies typically grow linearly with time, regardless of the system being integrable or not [27, 28], causing exponentially fast growth of complexity and with it a failure of these numerical methods. In our case though, see Fig.4, entropies grow much slower, namely in a power-law fashion

$$S^{(\#)} \sim t^{\beta}, \quad (6)$$

with  $\beta$  being less than 1. The most efficient simulations have been possible with density operators for small  $\mu$  where the exponent  $\beta$  is typically between 0.3 and 0.5.

## METHODS

The time evolution is performed by means of the tDMRG algorithm [29, 30]. In particular, for small  $\mu$  data (which is mostly reported here) the most efficient was the matrix product density operator version of tDMRG, with which we could reach times of the order  $t \simeq 200$  for system size  $n \simeq 2t$  using bond dimensions  $50 - 200$  resulting in relative truncation errors less than 1%. On the other hand, for  $\mu \approx 1$  (close to domain

wall pure state), the pure state version of tDMRG becomes more efficient as the corresponding entanglement entropy scaling exponents  $\beta$  are smaller. The two approaches appear to complement one another as can be seen in Fig.2(d). Neither approach allows us to observe long times in the intermediate region of  $\mu$ , where the exponents  $\beta$  become closer to 1.

In order to simulate the desired density operator by evolving pure states we define a set of initial states

$$|\Psi(t=0)\rangle = \bigotimes_{x<0} |\psi(\mu, \phi_x)\rangle \otimes \bigotimes_{x \geq 0} |\psi(-\mu, \phi_x)\rangle$$

where  $|\psi(\mu, \phi)\rangle = \sqrt{(1+\mu)/2} |\uparrow\rangle + e^{i\phi} \sqrt{(1-\mu)/2} |\downarrow\rangle$  is simply the Bloch sphere representation of a 2-level system and the  $\phi_x$  are uniform independent random numbers in the range  $[0, 2\pi)$ . The density matrix is then obtained as an ensemble average over a set of such pure random states  $\rho(t) = \mathbb{E}(|\Psi(t)\rangle\langle\Psi(t)|)$ . It is clear that an increasingly large set of random states is needed as the magnetisation approaches  $\mu \rightarrow 0$ , where the matrix product density operator simulation is favourable anyway.

- 
- [1] P. Calabrese, F. H. L. Essler and G. Mussardo, Special Issue on ‘Quantum Integrability in Out of Equilibrium Systems’, *J. Stat. Mech.* (2016), 064001 (2016).
  - [2] See, e.g. a review: E. Ilievski, M. Medenjak, T. Prosen and L. Zadnik, Quasilocl charges in integrable lattice systems, *J. Stat. Mech.* (2016), 064008 (2016).
  - [3] O. A. Castro-Alvaredo, B. Doyon and T. Yoshimura, Emergent hydrodynamics in integrable quantum systems out of equilibrium, *Phys. Rev. X* **6**, 041065 (2016).
  - [4] B. Bertini, M. Collura, J. De Nardis, M. Fagotti, Transport in out-of-equilibrium XXZ chains: exact profiles of charges and currents, *Phys. Rev. Lett.* **117**, 207201 (2016).
  - [5] D. Ruelle, Natural Nonequilibrium States in Quantum Statistical Mechanics, *J. Stat. Phys.* **98**, 57 (2000).
  - [6] D. Bernard and B. Doyon, Non-Equilibrium Steady-States in Conformal Field Theory, *Ann. Inst. Henri Poincaré* **16**, 113 (2015).
  - [7] J. Bhaseen, B. Doyon, A. Lucas and K. Schalm, Energy flow in quantum critical systems far from equilibrium, *Nature Physics* **11**, 509 (2015).
  - [8] M. Takahashi, Thermodynamics of One-Dimensional Solvable Models, Cambridge University Press (1999).
  - [9] A. Polkovnikov, K. Sengupta, A. Silva, and M. Vengalattore, Colloquium: Nonequilibrium dynamics of closed interacting quantum systems, *Rev. Mod. Phys.* **83**, 863 (2011).
  - [10] I. Bloch, J. Dalibard and S. Nascimbene, Quantum simulations with ultracold quantum gases, *Nature Physics* **8**, 267 (2012).
  - [11] J.-Y. Choi, et. al., Exploring the many-body localization transition in two dimensions, *Science* **352**, 1547 (2016).
  - [12] Z. Rieder, J. L. Lebowitz, and E. Lieb, Properties of a harmonic crystal in a stationary nonequilibrium state, *J. Math. Phys.* **8**, 1073 (1967).

- [13] H. Bethe, On the Theory of Metals, I. Eigenvalues and Eigenfunctions of a Linear Chain of Atoms, *Zeits. Physik* **74**, 205-226 (1931).
- [14] R. J. Baxter, Exactly Solved Models in Statistical Mechanics, (1982).
- [15] N. Hlubek, X. Zotos, S. Singh, R. Saint-Martin, A. Revcolevschi, B. Büchner, and C. Hess, Spinon heat transport and spin-phonon interaction in the spin-1/2 Heisenberg chain cuprates  $Sr_2CuO_3$  and  $SrCuO_2$ , *J. Stat. Mech.* **2012**, P03006 (2012).
- [16] X. Zotos, F. Naef, and P. Prelovšek, Transport and conservation laws, *Phys. Rev. B* **55**, 11029 (1997).
- [17] D. Gobert, C. Kollath, U. Schollwöck, and G. Schütz, Real-time dynamics in spin-1/2 chains with adaptive time-dependent density matrix renormalization group, *Phys. Rev. E* **71**, 036102 (2005).
- [18] I. G. Gochev, Contribution to the theory of plane domain walls in a ferromagnet, *Sov. Phys. JETP* **58**, 115 (1983).
- [19] T. Prosen, Open XXZ Spin Chain: Nonequilibrium Steady State and a Strict Bound on Ballistic Transport, *Phys. Rev. Lett.* **106**, 217206 (2011).
- [20] T. Prosen and M. Žnidarič, Matrix product simulation of non-equilibrium steady states of quantum spin chains, *J. Stat. Mech.* **2009**, P02035 (2009).
- [21] M. Žnidarič, Spin transport in a one-dimensional anisotropic Heisenberg model, *Phys. Rev. Lett.* **106**, 220601 (2011).
- [22] R. Steinigeweg and J. Gemmer, Density dynamics in translationally invariant spin-1/2 chains at high temperatures: A current-autocorrelation approach to finite time and length scales, *Phys. Rev. B* **80**, 184402 (2009).
- [23] C. Karrasch, J. E. Moore, and F. Heidrich-Meisner, Real-time and real-space spin and energy dynamics in one-dimensional spin-1/2 systems induced by local quantum quenches at finite temperatures, *Phys. Rev. B* **89**, 075139 (2014).
- [24] J. Sirker, R. G. Pereira, and I. Affleck, Conservation laws, integrability, and transport in one-dimensional quantum systems, *Phys. Rev. B* **83**, 035115 (2011).
- [25] R. Steinigeweg, J. Gemmer, W. Brenig, Spin-current autocorrelations from single pure-state propagation, *Phys. Rev. Lett.* **112**, 120601 (2014).
- [26] T. Prosen and I. Pižorn, Operator space entanglement entropy in a transverse Ising chain, *Phys. Rev. A* **76**, 032316 (2007).
- [27] P. Calabrese and J. Cardy, Evolution of entanglement entropy in one-dimensional systems, *J. Stat. Mech.* **2005** P04010 (2005).
- [28] G. De Chiara, S. Montangero, P. Calabrese, and R. Fazio, Entanglement entropy dynamics of Heisenberg chains, *J. Stat. Mech.* **2006**, P03001 (2006).
- [29] G. Vidal, Efficient simulation of one-dimensional quantum many-body systems, *Phys. Rev. Lett.* **93**, 040502 (2004).
- [30] U. Schollwöck, The density-matrix renormalization group in the age of matrix product states, *Annals of Physics* **326**, 96 (2011).

#### ACKNOWLEDGEMENTS

The authors would like to acknowledge support from ERC grant OMNES, as well as grants J1-7279, N1-0025, and P1-0044 of the Slovenian Research Agency.